Journal of Atmospheric and Solar-Terrestrial Physics 169 (2018) 1–5

Contents lists available at ScienceDirect

Journal of Atmospheric and Solar-Terrestrial Physics

journal homepage: www.elsevier.com/locate/jastp

Detecting atmospheric normal modes with periods less than 6 h by barometric observations

S.I. Ermolenko [a], G.M. Shved [a,*], Ch. Jacobi [b]

[a] Department of Atmospheric Physics, St. Petersburg State University, St. Petersburg, Russia
[b] Institute for Meteorology, University of Leipzig, Leipzig, Germany

ARTICLE INFO

Keywords:
Global atmospheric waves
Atmospheric normal modes
Earth's inner core oscillations

ABSTRACT

The theory of atmospheric normal modes (ANMs) predicts the existence of relatively short-period gravity-inertia ANMs. Simultaneous observations of surface air-pressure variations by barometers at distant stations of the Global Geodynamics Project network during an interval of 6 months were used to detect individual gravity-inertia ANMs with periods of ~2–5 h. Evidence was found for five ANMs with a lifetime of ~10 days. The data of the stations, which are close in both latitude and longitude, were utilized for deriving the phases of the detected ANMs. The phases revealed wave propagation to the west and increase of zonal wavenumbers with frequency. As all the detected gravity-inertia ANMs are westward propagating, they are suggested to be generated due to the breakdown of migrating solar tides and/or large-scale Rossby waves. The existence of an ANM background will complicate the detection of the translational motions of the Earth's inner core.

1. Introduction

To date, there is extensive knowledge about long-period atmospheric normal modes (ANMs) with periods of ~2–30 days (e.g., Madden, 2007). According to Longuet-Higgins (1968), these rotational ANMs, so-called Rossby waves, are named “Class-II” waves. Less comprehensively studied, however, are the relatively weak gravity-inertia ANMs belonging to “Class-I”. Therefore, the subject of this study is gravity-inertia ANMs.

Based on eigensolutions of Laplace's tidal equation for a barotropic ocean, a simple model of these ANMs results in wave periods less than 2 days (Hamilton and Garcia, 1986; Meyer and Forbes, 1997; Beliaev and Shved, 2014). The ANM amplitudes grow with height (e.g., Forbes, 1995). Hence, it may be suggested that some oscillations with the above mentioned periods, revealed in the middle and upper atmosphere, are gravity-inertia ANMs.

Above all, there are many observations of the oscillations with periods between ~6 and ~20 h in the mesosphere and lower thermosphere (MLT). First, those are wind measurements by radio wave reflection methods such as meteor radars (Forbes et al., 1999b; Portnyagin et al., 2000; Hocking, 2001) and partial reflection radars (Rüster, 1994; Fritts et al., 1998; Hoffmann et al., 2002; Kovalam and Vincent, 2003). Second, ground-based optical instruments have been used to observe airglow emissions from the mesopause region. Moreover, emission brightness, the observations of temperature and wind both derived from emission measurements show atmospheric oscillations with the abovementioned periods (Hernandez et al., 1993, 1997; Sivjee et al., 1994; Reisin and Scheer, 1996; Wu et al., 2002). Finally, these oscillations have been also detected by combined optical and radar measurements (Hernandez et al., 1992, 1996). The oscillation measurements in the MLT region were performed at the middle and high latitudes of both hemispheres. The lifetimes of the detected oscillations vary widely, up to about a month.

It is conceivable that gravity-inertia ANMs penetrate the middle and upper thermosphere. Accordingly, some of the oscillations with quasi-steady periods, observed there, may be attributed to them. The ANMs can account for the oscillations of the AE geomagnetic index in the 1–4 h period range (Bobova et al., 1990). The density variations near 200 km from the Satellite Electrostatic Triaxial Accelerometer experiment have shown oscillations with periods between 6 and 10 h (Forbes et al., 1999a). The incoherent scatter radar at Arecibo Observatory has detected oscillations with period ~1 h in the F-region during two ~35-h geomagnetically quiet observation periods (Livneh et al., 2007). Antarctic measurements of thermospheric airglow emissions during austral winter months have revealed non-tidal oscillations in the ~2–10 h period range with lifetimes from ~5 days to ~1 month (Gerrard et al., 2010).

It should be noted that the inertial effect for waves with periods of 2–5 h can be neglected. But since we will later draw some conclusions, involving waves with periods of more than 5 h (up to 20 h), we would like to keep the generalized name of the gravity-inertia normal modes

* Corresponding author.
E-mail address: g.shved@spbu.ru (G.M. Shved).

https://doi.org/10.1016/j.jastp.2017.12.007
Received 28 August 2017; Received in revised form 20 November 2017; Accepted 11 December 2017
Available online 19 December 2017

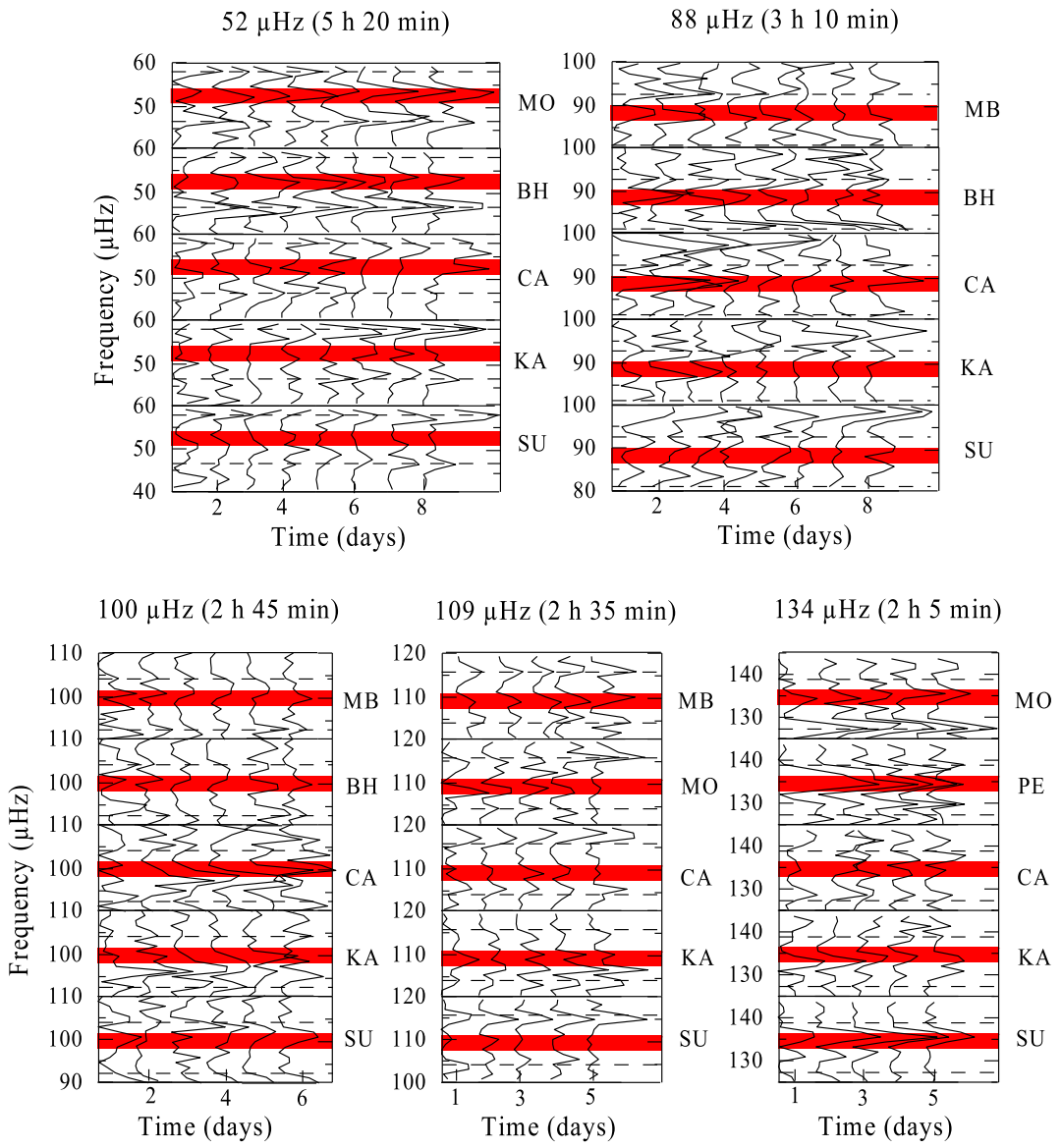

Fig. 1. Running spectra of the surface air-pressure for the station set, which show oscillations at the frequencies 52 μHz (from March 30 through April 11, 2009), 88 μHz (June, 14–25, 2009), 100 μHz (February 13–22, 2009), 109 μHz (from March 30 through April 5, 2009), and 134 μHz (April 6–12, 2009). The red bands display the frequency intervals around the oscillation frequencies considered. The periods of oscillations are given in parentheses. The dashed lines correspond to the frequencies of solar tide subharmonics.

here.

Meyer and Forbes (1997) first simulated gravity-inertia ANMs in the middle and upper atmosphere taking into account atmosphere non-isothermality, mean winds, and dissipation. Their 2D linearized perturbation model has shown eastward and westward waves for zonal wavenumbers 1–3 and periods up to ~5 h. The eastward and westward waves for zonal wavenumber 0–4 and periods of ~9–12 h have been also simulated with a numerical spectral model (Mayr et al., 2004; Talaat and Mayr, 2011).

As to the measurements of the gravity-inertia ANMs in the lower atmosphere, Hamilton and Garcia (1986) have reported waves up to a period of ~11 h by using surface air-pressure observations in the tropics. In addition to barometer measurements, oscillations of the lower atmosphere can also be detected by seismometers and gravimeters (Shved et al., 2013). However, no method has so far revealed an individual oscillation with period less than ~11 h in the lower atmosphere. Nevertheless, signatures of gravity-inertia ANMs were detected in the ~1–5 h period range. This has been made possible by observing clustering of the ANMs on the frequency axis, with equal intervals between the clusters in this period range (Beliaev and Shved, 2014). Such an interval has been revealed by both barometer and seismometer measurements (Petrova and Shved, 2000; Karpova et al., 2004; Shved et al., 2015). Also, it has been noted that in the ~1–2 h period range the amplification of surface air-pressure perturbations (Fig. 11a in (Livneh et al., 2007)) corresponds to the discrete spectrum of oscillations detected by seismometer (Petrova and Shved, 2000).

The purpose of the present study is to reveal individual ANMs in the ~2–5 h period range from barometer measurements using a network of observation stations. We shall analyze ANM events with lifetimes of several days simultaneously observed at stations spaced even very far. The remainder of the paper is organized as follows: In Section 2 the observational basis is described. The analysis method is presented in section 3. In section 4 the results will be presented and discussed, and section 5 concludes the paper.

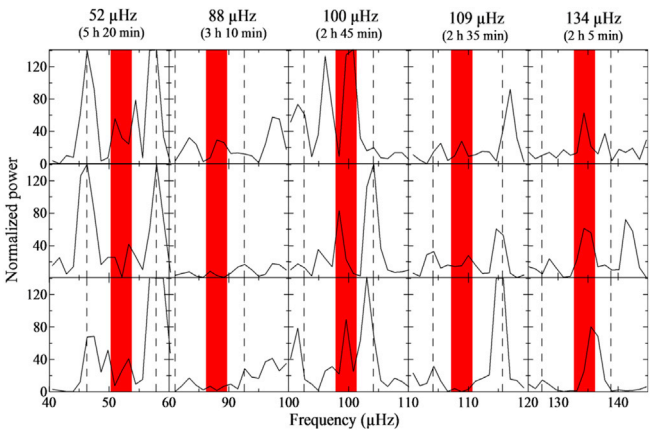

Fig. 2. Cross-spectra of cross-covariances between the surface air-pressure measurements at the MO station and the stations of CA (top), KA (middle), and SU (bottom), performed during the periods of existence of the oscillations revealed and shown in Fig. 1. The red bands display the frequency intervals around the oscillation frequencies considered. The dashed lines correspond to the frequencies of solar tide subharmonics.

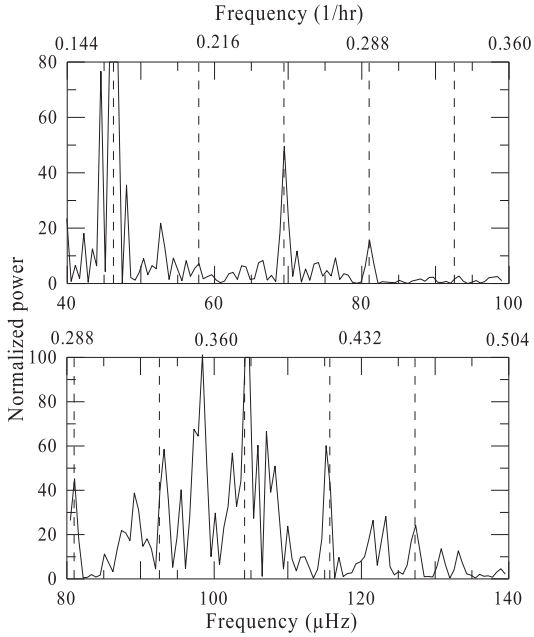

Fig. 3. Cross-spectra of cross-covariances between the surface air-pressure measurements at the stations of MO and CA for a whole two-year interval. It is used the filtered series at the cutoff frequencies of 40 μHz (top) and 80 μHz (bottom). The dashed lines correspond to the frequencies of solar tide subharmonics.

2. Observational data

We utilized barometer data from the Global Geodynamics Project (GGP) network (Crossley and Hinderer, 2009). The barometer sensitivity is high, up to $\sim 10^{-1}$ Pa. The surface air-pressure measurements are presented in the GGP database with a 1-min step. Data from the following GGP stations have been chosen for analysis. First of all, four stations at very similar latitude in Central Europe have been selected to obviate a possible falling of anyone of them on an ANM node, where there is no pressure oscillation. These sites are Membach (MB, 50.6°N, 6.0°E), Bad Homburg (BH, 50.2°N, 8.6°E), Moxa (MO, 50.6°N, 11.9°E), and Pecny (PE, 49.9°N, 14.8°E). Furthermore, two stations have been selected at longitudes close to the MO longitude, but on other latitudes, namely Medicina (MC, 44.5°N, 11.6°E) in Southern Europe and Ny-Alesund (NY, 78.9°N, 11.9°E) on Svalbard. Two stations at longitudes very much different from the European ones have also been selected to test the global nature of observed oscillations; these are Cantley (CA, 45.6°N, 75.8°W) in Canada and Kamioka (KA, 36.4°N, 137.3°E) in Japan. Finally, to test the possible penetration of ANMs into the Southern hemisphere, the Sutherland (SU, 32.4°S, 20.8°E) observations have been used. We analyzed measurements obtained during a half-year interval (January 16 through July 17, 2009), except for the NY data. This dataset ranges from April 26 through July 7, 2009.

3. Analysis method

The processing of the barometer series and its evaluation are given in detail by Shved et al. (2015). Here we only briefly repeat the main elements of the method. Lomb-Scargle spectra are calculated for the series, which before have been filtered at the cutoff frequencies of 40, 80, and 120 μHz. The transience of ANMs has demanded spectral analyses for relatively short 5-day segments of the half-year series. The spectral power in the periodograms is presented at a resolution of 1.16 μHz. The statistical significance of the spectral peaks was estimated by comparing the resulting spectra with a white noise spectrum. We took into account spectral peaks with a 90% confidence level.

The ANM transience and local features of the measurements and/or meteorological conditions suggest that the oscillations detected can vary in frequency. We allow a frequency variation within three 1.16-μHz intervals. As the considered ANMs are very weak, a set of requirements is defined to be confident that an oscillation detected is ANM:

1. The 1.16-μHz intervals involving solar tide subharmonics and both neighboring intervals are excluded from the analysis.
2. We only take into account oscillations that are simultaneously observed at all the four Central European stations in a sequence of at least three 5-day spectra.
3. The oscillation must be simultaneously observed in the same observational period at least at one of the stations CA, KA, or SU.
4. An oscillation is believed to be an ANM if they are visible in the cross-covariances between the measurement series of a Central European station and the CA and/or KA stations.

To obtain the cross-spectra, series of 10-day length centered around the time interval of detected ANMs have been used. These cross-covariances were analyzed for a maximal lag time of 5 days.

The way to confirm that the oscillations detected are global is to reveal their frequencies in cross-spectra based on long series of barometer measurements at far-spaced stations. This is why the cross-spectra for a whole two-year interval with maximal lag time of 10 days have been calculated for the measurement at the stations of MO and CA.

Zonal wavenumbers of the detected ANMs have been calculated from the phases of relevant oscillations at the four Central European stations. First, a high-pass filter with a cutoff frequency close to the ANM ones has been applied to the initial series. Then, the series derived have been subjected to narrow band filtering to reveal the sinusoids at the ANM frequencies in the band with width of 1.16 μHz. Further, a time interval has been found, in which the sinusoids for all four stations are best represented. ANM phases at the longitudes of the stations have been derived from the sinusoids for this interval. The wavelength has been detected from the phase change with longitude through least-squares fitting. To improve the fit, the data point with the largest deviation from the fit has been rejected and the fitting was repeated.

4. Results and discussion

We have detected five cases that have met all the requirements. Fig. 1 shows running spectra for these cases, while the detected cross-spectra for those time intervals are presented in Fig. 2. Two ANMs with

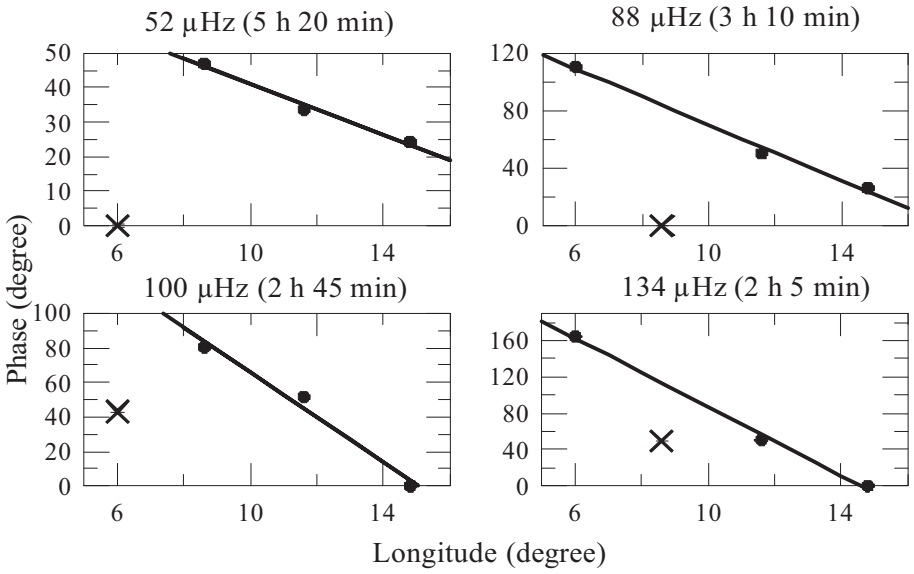

Fig. 4. Phase progressions of the revealed oscillations (see Fig. 1) observed at the Central European stations as functions of longitude. The thick line is a linear fit to the three phase data points. The phase point excluded from the fit is given by cross.

frequencies of about 52 and 88 μHz (periods about 5 h 20 min and 3 h 10 min, respectively) were observed over eight 5-day intervals (12 days in total). Three ANMs with frequencies about 100, 109, and 134 μHz (periods about 2 h 45 min, 2 h 35 min, and 2 h 5 min, respectively) were observed over six 5-day intervals (10 days in total) for the first frequency and over three intervals (7 days) for the other ones.

The running spectra (Fig. 1) and cross-spectra (Fig. 2) show the oscillations at frequencies of 52, 100, and 134 μHz at all the far-spaced stations simultaneously. In addition to Europe, the 109-μHz oscillation signatures were also observed at CA and KA. As to the 88-μHz oscillation, it was additionally observed with confidence at CA only. The absence of reliable detection of the 88- and 109-μHz oscillations at KA can be presumably explained by local features of measurements and/or meteorological conditions. This is also the case for SU, which may be explained on the basis of global observations of Rossby waves. Meteor radar observations of these waves with periods of ~2–~16 days, performed simultaneously in the Northern and Southern hemispheres, show that there are episodes when a wave does not penetrate from one hemisphere to the other (Tunbrige and Mitchell, 2009; Day and Mitchell, 2010a, 2010b; Fritts et al., 2012; Iimura et al., 2015). We suggest that the same may be true for gravity-inertia ANMs.

Fig. 3 presents the cross-spectra for the 2-year interval (January 1 of 2009 through December 31 of 2010) of measurements at far-spaced stations. All the ANMs detected appear in these spectra along with the solar tidal subharmonics. The absence or weakness of some subharmonics is most likely due to the proximity of the latitude of one or both stations to the latitude of pressure oscillation node. It can be seen in Fig. 3 that there are also ANM signatures at other frequencies, which, however, have not been identified with confidence in this study.

In the considered period range the gravity waves (GWs) are observed in the atmosphere (e.g., Fritts and Alexander, 2003; Plougonven and Zhang, 2014). The oscillations revealed here are not GWs for the following reasons. First of all, the duration of GW wave packets, as a rule, does not exceed the order of ten GW periods. Since the spectral analysis was performed for the 5-day series, first, the detection of GWs is unlikely. Second, the lifetime of the revealed oscillations is of ~10 days, which is much more than GW packet duration. Moreover, there are no narrow frequency intervals for the predominant occurrence of GWs: the probabilities of GW generation are smooth functions of frequency. In contrast to the GWs, as indicated in the Introduction, the gravity-inertia ANMs are grouped in frequency, with the periodicity of ~6 μHz being revealed for the GW clusters in the ~1–5 h period range (Shved et al., 2015). The cross-spectra in Fig. 3 show fairly narrow peaks between tidal subharmonic frequencies.

An attempt was made to determine the zonal wavenumbers s of the detected ANMs (Fig. 4). Those have been found to be westward waves with zonal wavenumbers $s = 4 \pm 2$, 10 ± 5, 12 ± 8, and 16 ± 7 for the ANM frequencies of 52, 88, 100, and 134 μHz, respectively. The strong uncertainty of s for each frequency can be explained by simultaneous generation of a set of ANMs at close frequencies, which is allowed by theory (Beliaev and Shved, 2014). The superposition of ANMs with close frequencies is the most plausible hypothesis, why the computational code did not give any linear fit for the 109 μHz oscillation. All of the previous observations of propagation direction for gravity-inertia ANMs showed westward direction as well (Hernandez et al., 1992, 1993, 1996, 1997; Forbes et al., 1999a, 1999b; Portnyagin et al., 2000; Kovalam and Vincent, 2003). According to the gravity-inertia ANM theory, the westward direction is not preferred to the eastward one (Meyer and Forbes, 1997; Mayr et al., 2004; Beliaev and Shved, 2014). Therefore, the observations of only westward propagating ANMs should be owing to their origin. As both the migrating solar thermal tides and large-scale Rossby waves propagate to the west and belong to the strongest global waves, their breakdown may be suggested as a dominant excitation source for the observed gravity-inertia ANMs. An increase of the amplitude of the tides and Rossby waves with height (e.g., Forbes, 1995) results in nonlinear processes which break down these global waves and generate ones with other periods in the middle and upper atmosphere. For example, it is shown that in MLT the terdiurnal tides originate from nonlinear interactions between diurnal and semidiurnal tides (Guharay et al., 2013; Moudden and Forbes, 2013), and the interactions of the 6-day Rossby wave with solar tides result in secondary waves (Forbes and Zhang, 2017).

According to theory, the range of possible wavenumbers s increases with ANM frequency (Beliaev and Shved, 2014). Moreover, there is a physical consideration which explains the s increase in the detected ANM with frequency. Namely, it may be assumed that the ANMs with zonal phase speeds that do not exceed the speed of sound are predominantly generated. The wavenumber corresponding to a phase speed closest to the speed of sound increases with wave frequency. As a suitable example, for the Central European station latitudes such s are 4, 7, 9, and 11 for the wave frequencies of 52, 88, 100, and 134 μHz, respectively. Observations of ANMs with period up to ~6 h (Forbes et al., 1999a) have revealed zonal wavenumbers up to $s = 6$. This result and the s values derived in the present study are in agreement with ANM theory and the above physical consideration.

5. Conclusions

The barometer observations at far-spaced stations, performed simultaneously during semi-annual interval, for the first time have revealed individual non-tidal global atmospheric oscillations in the ~2–5 h period range. These oscillations have a lifetime of ~10 days and are most likely gravity-inertia normal modes or "Lamb" waves. In accordance both with the theory of these normal modes and with limiting the phase speed of waves to the speed of sound, the zonal wavenumbers of the waves detected increase with wave frequency. Like the normal modes revealed in the ~6–20 h period range in previous investigations, the waves propagate to the west. We suggest that the short-period gravity-inertia normal modes are mainly generated due to the breakdown of solar thermal tides and/or large-scale Rossby waves, which both propagate to the west as well.

The translational motions of the Earth's inner core (Slichter triplet) presumably have periods in the 3–10 h range (e.g., Rosat et al., 2004). As seismometers and gravimeters detect atmospheric oscillations in this period range, it should be assumed that the existence of atmospheric normal mode background will complicate the detection of the Slichter mode.

Acknowledgments

Barometer data have been kindly provided by through the GGP project. S.I. Ermolenko acknowledges support by the German-Russian Interdisciplinary Science Center (G-RISC) funded by the German Federal Foreign Office via the German Academic Exchange Service (DAAD). We would like to thank an anonymous reviewer for comments which significantly helped to improve the manuscript.

References

Beliaev, T.M., Shved, G.M., 2014. Short-period normal modes of the atmosphere. Izv. Atmos. Ocean. Phys. 50, 562–568.
Bobova, V.P., Osypov, K.S., Savina, N.G., Vladimirsky, B.M., Pudovkin, M.I., 1990. Probability of the seismic origin of long-period (T = 1–4 h) variations of geomagnetic disturbances. Geomagn. Aeron. 30, 492–494.
Crossley, D., Hinderer, J., 2009. A review of the GGP network and scientific challenges. J. Geodyn. 48, 299–304.
Day, K.A., Mitchell, N.J., 2010a. The 16-day wave in the Arctic and Antarctic mesosphere and lower thermosphere. Atmos. Chem. Phys. 10, 1461–1472.
Day, K.A., Mitchell, N.J., 2010b. The 5-day wave in the Arctic and Antarctic mesosphere and lower thermosphere. J. Geophys. Res. 115, D01109 https://doi.org/10.1029/2009JD012545.
Forbes, J.M., 1995. Tidal and planetary waves. In: Johnson, R.M., Killeen, T.L. (Eds.), The Upper Mesosphere and Lower Thermosphere: a Review of Experiment and Theory. Geophys. Monogr, vol. 87. AGU, Washington, D. C., pp. 67–87
Forbes, J.M., Palo, S.E., Marcos, F.A., 1999a. Longitudinal structures in lower thermosphere density. J. Geophys. Res. 104, 4373–4385.
Forbes, J.M., Palo, S.E., Zhang, X., Portnyagin, YuI., Makarov, N.A., Merzlyakov, E.G., 1999b. Lamb waves in the lower thermosphere: observational evidence and global consequences. J. Geophys. Res. 104, 17,107–17,115.
Forbes, J.M., Zhang, X., 2017. The quasi-6 day wave and its interactions with solar tides. J. Geophys. Res. 122A, 4764–4776. https://doi.org/10.1002/2017JA023954.
Fritts, D.C., Riggin, D.M., Balsley, B.B., Stockwell, R.G., 1998. Recent results with an MF radar at McMurdo, Antarctica: characteristics and variability of motions near 12-hour period in the mesosphere. Geophys. Res. Lett. 25, 297–300.
Fritts, D.C., Alexander, M.J., 2003. Gravity wave dynamics and effects in the middle atmosphere. Rev. Geophys. 41, 1003. https://doi.org/10.1029/2001RG000106. Correction, **50**, 2012, 3004, https://doi.org/10.1029/2012RG000409.
Fritts, D.C., Iimura, H., Lieberman, R., Janches, D., Singer, W., 2012. A conjugate study of mean winds and planetary waves employing enhanced meteor radars at Rio Grande, Argentina (53.8°S) and Juliusruh, Germany (54.6°N). J. Geophys. Res. 117, D05117 https://doi.org/10.1029/2011JD016305.
Gerrard, A.J., Detrick, D., Mende, S.B., Lanzerotti, L.J., Weatherwax, A.T., Bhattacharya, Y., 2010. Photometric observations of 630.0-nm OI and 427.8-nm N_2^+ emission from South Pole and McMurdo stations during winter: analysis of temporal variations spanning minutes to hourly timescales. J. Geophys. Res. 115, A08231 https://doi.org/10.1029/2009JA014970.
Guharay, A., Batista, P.P., Clemesha, B.R., Sarkhel, S., Buriti, R.A., 2013. On the variability of the terdiurnal tide over a Brazilian equatorial station using meteor radar observations. J. Atmos. Sol. Terr. Phys. 104, 87–95.
Hamilton, K., Garcia, R.R., 1986. Theory and observations of the short-period normal mode oscillations of the atmosphere. J. Geophys. Res. 91, 11,867–11,875.
Hernandez, G., Smith, R.W., Fraser, G.J., Jones, W.L., 1992. Lange-scale waves in the upper mesosphere at Antarctic high latitudes. Geophys. Res. Lett. 19, 1347–1350.
Hernandez, G., Fraser, G.J., Smith, R.W., 1993. Mesospheric 12-hour oscillation near south pole, Antarctica. Geophys. Res. Lett. 20, 1787–1790.
Hernandez, G., Forbes, J.M., Smith, R.W., Portnyagin, YuI., Booth, J.F., Makarov, N., 1996. Simultaneously mesospheric wind measurements near South Pole by optical and meteor radar methods. Geophys. Res. Lett. 23, 1079–1082.
Hernandez, G., Smith, R.W., Kelley, J.M., Fraser, G.J., Clark, K.C., 1997. Mesospheric standing waves near South Pole. Geophys. Res. Lett. 24, 1987–1990.
Hocking, W.K., 2001. Middle atmosphere dynamical studies at Resolute Bay over a full representative year: mean winds, tides, and special oscillations. Radio Sci. 6, 1795–1822.
Hoffmann, P., Singer, W., Keuer, D., 2002. Variability of the mesospheric wind field at middle and Arctic latitudes in winter and its relation to stratospheric circulation disturbances. J. Atmos. Sol. Terr. Phys. 64, 1229–1240.
Iimura, H., Fritts, D.C., Janches, D., Singer, W., Mitchell, N.J., 2015. Interhemispheric structure and variability of the 5-day planetary wave from meteor radar wind measurements. Ann. Geophys. 33, 1349–1359.
Karpova, N.V., Petrova, L.N., Shved, G.M., 2004. Atmospheric and earth surface oscillations with steady frequencies in the 0.7–1.5 and 2.5–5.0 h period ranges. Izv., Atmos. Ocean. Phys. 40, 13–24.
Kovalam, S., Vincent, R.A., 2003. Intradiurnal wind variations in the midlatitude and high-latitude mesosphere and lower thermosphere. J. Geophys. Res. 108, D04135 https://doi.org/10.1029/2002JD002500.
Livneh, D.J., Seker, I., Djuth, F.T., Mathews, J.D., 2007. Continuous quasiperiodic thermospheric waves over Arecibo. J. Geophys. Res. 112, A07313 https://doi.org/10.1029/2006JA012225.
Longuet-Higgins, M.S., 1968. The eigenfunctions of Laplace's tidal equations over a sphere. Philos. Trans. R. Soc. London, Ser. A 262, 511–607.
Madden, R.A., 2007. Large-scale, free Rossby waves in the atmosphere: an update. Tellus 59A, 571–590.
Mayr, H.G., Mengel, J.G., Talaat, E.R., Porter, H.S., Chan, K.L., 2004. Properties of internal planetary-scale inertio gravity waves in the mesosphere. Ann. Geophys. 22, 3421–3435.
Meyer, C.K., Forbes, J.M., 1997. Natural oscillations of the ionosphere-thermosphere-mesosphere (ITM) system. J. Atmos. Sol. Terr. Phys. 59, 2185–2202.
Moudden, Y., Forbes, J.M., 2013. A decade-long climatology of terdiurnal tides using TIMED/SABER observations. J. Geophys. Res. 118A, 4534–4550. https://doi.org/10.1002/jgra.50273.
Petrova, L.N., Shved, G.M., 2000. Revealing short-period global oscillations of the atmosphere from seismic observations. Izvestiya Atmos. Ocean. Phys. 36, 64–68.
Plougonven, R., Zhang, F., 2014. Internal gravity waves from atmospheric jets and fronts. Rev. Geophys. 52, 33–76. https://doi.org/10.1002/2012RG000419.
Portnyagin, Y.I., Forbes, J.M., Merzlyakov, E.G., Makarov, N.A., Palo, S.E., 2000. Intradiurnal wind variations observed in the lower thermosphere over the South Pole. Ann. Geophys. 18, 547–554.
Reisin, E.R., Scheer, J., 1996. Characteristics of atmospheric waves in the tidal period range derived from zenith observations of $O_2(0-1)$ Atmospheric and OH(6−2) airglow at lower midlatitudes. J. Geophys. Res. 101, 21,223–21,232.
Rosat, S., Hinderer, J., Crossley, D., Boy, J.P., 2004. Performance of superconducting gravimeters from long-period seismology to tides. J. Geodyn. 38, 461–476.
Rüster, R., 1994. VHF radar observations of nonlinear interactions in the summer polar mesosphere. J. Atmos. Terr. Phys. 56, 1289–1299.
Shved, G.M., Ermolenko, S.I., Karpova, N.V., Wendt, S., Jacobi, Ch, 2013. Detecting global atmospheric oscillations by seismic instruments. Izv. Phys. Solid Earth 49, 278–288.
Shved, G.M., Ermolenko, S.I., Hoffmann, P., 2015. Revealing short-period normal modes of the atmosphere. Izv. Atmos. Ocean. Phys. 51, 498–504.
Sivjee, G.G., Walterscheid, R.I., McEwen, D.J., 1994. Planetary wave disturbances in the Arctic winter mesopause over Eureka (80°N). Planet. Space Sci. 42, 973–986.
Talaat, E.R., Mayr, H.G., 2011. Model of semidiurnal pseudo-tide in the high-latitude upper mesosphere. J. Atmos. Sol. Terr. Phys. 73, 2386–2391.
Tunbrige, V.M., Mitchell, N.J., 2009. The two-day wave in the Antarctic and Arctic mesosphere and lower thermosphere. Atmos. Chem. Phys. 9, 6377–6388.
Wu, Q., Killeen, T.L., McEwen, D., Solomon, S.C., Guo, W., Sivjee, G.G., Reeves, J.M., 2002. Observation of the mesospheric and lower thermospheric 10-hour wave in the northern polar region. J. Geophys. Res. 107, A61082 https://doi.org/10.1029/2001JA000192.